Adsorption Kinetics of Diblock Copolymers from a Micellar Solution on Silica and Titania

H. D. Bijsterbosch, M. A. Cohen Stuart,* and G. J. Fleer

Laboratory for Physical Chemistry and Colloid Science, Wageningen Agricultural University, Dreijenplein 6, 6703 HB Wageningen, The Netherlands

Received December 9, 1997; Revised Manuscript Received September 14, 1998

ABSTRACT: The solution and adsorption behavior of a series of diblock copolymers of hydrophobic poly(dimethyl siloxane) and hydrophilic poly(2-ethyl-2-oxazoline) was studied. These block copolymers formed large polydisperse micelles in an aqueous solution. The critical micelle concentration was lower than 2 mg L^{-1}. The adsorption kinetics of these polymers onto macroscopically flat oxide surfaces was studied with reflectometry in stagnation point flow. Both blocks of the copolymers had affinity for silica, and only the hydrophobic block had affinity for the titania surface. Nevertheless, the adsorption curves on silica and titania had similar features. The adsorption kinetics was affected by the exchange rate between micelles and free polymers. For short polymer chains the exchange rate was fast compared with the time necessary for diffusion across the diffusive layer. Before the micelles arrived at the surface, they had already broken up into unimers. Because the critical micelle concentration was very low, the experimental adsorption rate was determined by the diffusion of micelles toward the surface. This was not the case for the longest polymer chain; the exchange between micelles and unimers was relatively slow. The micelles did not adsorb directly, and the adsorption rate was determined by the exchange of polymers between micelles and solution. For all polymer samples the adsorption increases linearly as a function of time, up to very high adsorbed amounts where it reaches a plateau. The adsorbed amount on silica is considerably higher than found for titania. The poly(dimethyl siloxane) was anchored more strongly to the silica surface than to titania; the density of the adsorbed layer could therefore become higher.

Introduction

Polymers play an important role in many natural and technical processes. Their interfacial behavior especially can have an enormous impact on the properties of materials.[1] For example, polymers are known for their ability to stabilize colloidal dispersions.[2] This steric stabilization can be achieved when the polymers adsorb on the surface of the colloidal particles and form a layer that is thick enough to overcome the attractive van der Waals force. The thickness of the layer is determined mainly by the number and the length of the polymer chain ends (tails) protruding into the solution. For a thick and stabilizing layer long tails are required, which have to be firmly anchored to the surface. In diblock copolymers these conditions can be met by using two different blocks where one block (*the anchor*) has a high affinity for the surface and the other block (*the buoy*) protrudes far into the solution in the form of a long tail. The adsorption of block copolymers has been extensively studied theoretically[3−8] as well as experimentally.[9−17]

The solvent plays an important role in the adsorption of block copolymers. If both blocks of the diblock copolymer are soluble, the solvent is called nonselective. If, however, only one of the blocks dissolves and the other does not, the solvent is selective, and the block copolymers may form micelles. Very thick layers can be built up in both types of solvents, with the nonadsorbing block forming a dilute and extended buoy layer. In a nonselective solvent the anchor layer is swollen because of the presence of solvent molecules. In a selective solvent in which the nonsoluble block is the anchor, the anchor layer is thin and dense because the solvent is expelled. In both types of solvent a maximum in the adsorbed amount is found as a function of the block copolymer composition. When the polymer chains are long, this maximum will be found for a relatively short anchor block. The anchor block is then just long enough to keep the whole molecule attached to the surface, and the relatively long tails can form a very extended dense layer, a so-called *brush*.[18] However, when in a selective solvent the soluble block is preferentially adsorbed, an adsorbed layer of micelles or a bilayer may be formed. In the bilayer the soluble blocks are expected to form a swollen adsorbed layer close to the wall. A second, very dense layer may then be formed by the nonsoluble blocks. Further away from the surface another layer of soluble blocks is thought to be built up, minimizing the contacts between the solvent and the nonsoluble block.[5] For a layer of adsorbed micelles the dense middle layer is not continuous, and we may expect lateral inhomogeneities for that situation. A schematic presentation of possible structures of the adsorbed layer is given in Figure 1.

The structures sketched for the adsorbed layer of block copolymers are those corresponding to equilibrium states. However, kinetic barriers can make it difficult or even impossible to reach this equilibrium state. In a nonselective solvent the osmotic pressure in the dense brush forms a barrier, which makes it hard for additional polymer molecules to adsorb because they first have to diffuse through this brush. It can therefore take a very long time before equilibrium is reached. In a selective solvent where only the nonsoluble block has affinity for the surface, an extra barrier is formed by the existence of a micellar corona of soluble blocks, which is repelled by the surface. The hydrophobic blocks then have to diffuse over a long distance through a nonfavorable environment before they reach the surface. For such a system it may even take more time to reach the equilibrium state than for the adsorption from a nonselective solvent.

10.1021/ma971793l CCC: $15.00
Published on Web 12/03/1998

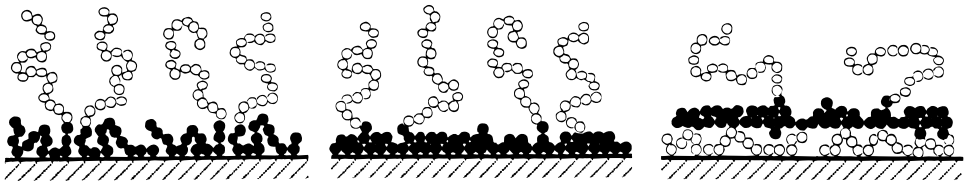

Figure 1. Possible structures of an adsorbed diblock copolymer layer. In the left-hand side, the anchor blocks (filled circles) are soluble and form a swollen layer, the nonadsorbing buoy blocks (open circles) protrude into the solution. In the middle picture, the anchor blocks are not soluble and form a melt at the surface. In the right-hand side, a (laterally homogeneous) bilayer is formed with a swollen anchor layer, a dense nonsoluble middle layer, and a layer of buoy blocks. In this case the soluble blocks (open circles) form both the anchor and the buoy layer.

The kinetics of diblock copolymer adsorption are very important, especially for industrial purposes, where the time available for different processes is limited and nonequilibrium conditions may prevail. Obviously, in the study of block copolymer adsorption attention should not only be paid to the equilibrium state but also to the kinetics.

In this article we consider the adsorption of amphiphilic diblock copolymers from an aqueous solution onto silicon dioxide (silica or SiO_2) and titanium dioxide (titania or TiO_2) surfaces. A series of four diblock copolymers of poly(dimethyl siloxane) (PDMS) and poly(2-ethyl-2-oxazoline) (PEtOx) was used. The block copolymers form micelles in solution. It turns out that both blocks have affinity for silica, but only the hydrophobic block (PDMS) has affinity for the titania surface. The equilibrium adsorbed state for both surfaces is expected to be as drawn in the middle panel of Figure 1. However, before this equilibrium is attained, the structures of the adsorbed layers on silica and titania can be different. The adsorption onto silica probably proceeds by an intermediate structure of adsorbed micelles, because the corona has affinity for silica. When finally, by rearrangement of the micelles, the hydrophobic core has made contact with the surface, a saturated block copolymer layer may be formed in which the surface is completely covered by a dense layer of hydrophobic blocks and the hydrophilic chains protrude into the solution.

A steric barrier must be overcome for adsorption of the micelles on titania; the micelle must bring its core into contact with the surface but is hindered by the existence of a nonadsorbing corona. Johner and Joanny[7] used scaling arguments to show that the potential barrier of the corona is very high and that formation of the surface layer in this case proceeds by the attachment of free polymer chains or unimers, i.e., polymer molecules that are not in micelles. The micelles act as a source that supplies unimers to the solution from which they can adsorb to the surface. Eventually, the adsorbed layer will probably be similar to that on silica. For the kinetics of adsorption the exchange rate between micelles and unimers is thus very important. The micelles can only act as a source for new unimers when the exchange rate is relatively fast compared with the time the micelle is near the adsorbing surface. The exchange rate depends on many qualities among which are the solvent quality, the flexibility of the core, and the polymer block lengths. In our experimental system we used a series of four diblock copolymers differing in total length but with a constant weight ratio between hydrophilic and hydrophobic blocks. Within this series, the exchange rates of unimer molecules between micelles and solution strongly depend on the total polymer length. The molar mass of the largest polymer is 40 times higher than that of the smallest polymer. This will probably lead to micellar relaxation times that differ by several orders of magnitude.[19] For the purpose of this study we hope that the shortest polymer chains have a micellar relaxation time that is fast compared with the contact time with the surface, whereas that of the largest polymer molecules is much slower. Investigating the adsorption kinetics as a function of molar mass can give us more insight into the mechanism of diblock copolymer adsorption.

Micellar solutions of the polymers in water were characterized using dynamic light scattering and cryogenic transmission electron microscopy. The adsorption of these polymers onto macroscopically flat oxide surfaces was studied with reflectometry in the so-called stagnation point of an impinging jet flow cell. We were able to follow the time-dependent adsorption up to several hours after the onset of the experiment. For a comparison between the experimental adsorption rate and the theoretical flux of polymers toward the surface, it is necessary to know the flow pattern in the flow cell. Before discussing the experimental results, we will calculate in the next section the flux of polymer molecules toward the surface, in particular in the stagnation point. A new feature in this treatment is the inclusion of the exchange of unimers between micelles and solution.

Convective Diffusion of Polymer in a Stagnation Point Flow

We want to know the flow behavior of the solution in the experimental setup and the resulting flux toward the surface under investigation. In the reflectometer used to measure the adsorption of the polymer, we have an impinging jet flow which was described extensively by Dabros and Van de Ven.[20] A schematic presentation of an impinging jet flow is given in Figure 2.

The mass transport of particles in diluted suspensions toward the surface in the stagnation point of an impinging jet flow was calculated in detail by Dabros and Van de Ven.[20] When we consider the polymer coils in solution as particles, the same expressions hold for the flux of polymer molecules toward the surface in a stagnation point. The flow velocity vector near $r = 0$ can be written in cylindrical coordinates:

$$\bar{v} = \begin{pmatrix} v_r \\ v_z \\ v_\phi \end{pmatrix} = \begin{pmatrix} \alpha z r \\ -\alpha z^2 \\ \beta r z \end{pmatrix} \tag{1}$$

where α and β are streaming intensity parameters. These also can be expressed as $\bar{\alpha}U/R^2$ and $\bar{\beta}U/R^2$, respectively, where U is the mean velocity in the tube at the outlet plane ($z = h$), and $\bar{\alpha}$ and $\bar{\beta}$ are dimension-

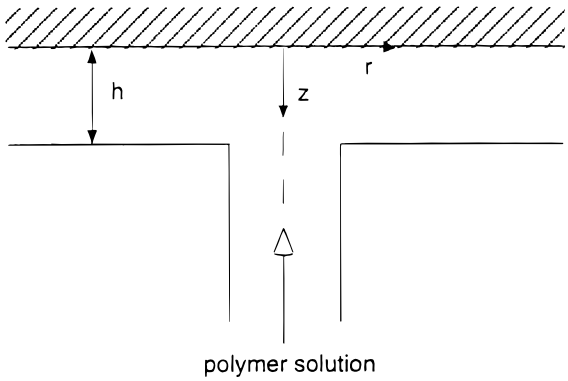

Figure 2. The geometry of the impinging jet flow cell. The polymer solution flows through the inlet tube with radius R, and enters the gap between two parallel surfaces separated by a distance h. The stagnation point is located at the top surface on the axis of symmetry (dotted line). The distance from that surface is z, and the radial distance to the axis of symmetry is r.

less streaming intensity parameters. The value of these parameters depends on the Reynolds number Re and on the geometric factors h and R; the value can be found numerically.[20] The Reynolds number is related to the mean velocity, the radius of the tube, and the kinematic viscosity ν through $Re = UR/\nu$. For an impinging jet flow $\vec{\beta} = 0$, for symmetry reasons. The total concentration c of polymer in the solution satisfies the continuity equation:

$$\frac{\partial c_i}{\partial t} = -\vec{\nabla}\cdot\vec{F}_i + S_i(t) = -\vec{\nabla}\cdot((c_i\vec{v}) - (D_i\nabla\vec{c}_i)) + S_i(t) = -\vec{v}\nabla\vec{c}_i + D_i\vec{\nabla}^2 c_i + S_i(t) = 0 \quad (2)$$

where the subscript i indicates the polymeric species, i.e., i = u for unimers and i = m for micelles, t is time, $\vec{F}_i$ is the flux vector, and $\vec{\nabla}$ denotes the gradient operator. The flux has a convective term $c_i\vec{v}$, where $\vec{v}$ is the velocity vector, and a diffusive term $-D_i\nabla\vec{c}_i$, where D is the diffusion coefficient. We only consider incrompressible fluids, i.e., $c_i\nabla\cdot\vec{v} = 0$, and stationary states, i.e., $\partial c_i/\partial t = 0$. The total flux of polymer is given by the sum of the fluxes for unimers and micelles, the concentrations of which are coupled through the exchange of polymers between micelles and solution. This exchange is included as the source term $S_i(t)$, for which we can write:

$$S_u(t) = -S_m(t) = -k_s^- c_m + k_s^+ (c_u)^N \quad (3)$$

The rate constants k_s^+ and k_s^- determine the "on-and-off" rate of micelle formation, and N is the number of unimers per micelle. For the sake of clarity, we only consider two limits: the exchange is very slow or, conversely, very fast compared with the time the micelles need to diffuse across the diffusive layer (of thickness δ_m) toward the surface.

Slow Exchange Rate

First, we consider that the exchange rate between unimers and micelles is very slow. The time τ_r a micelle needs for break up is then long compared with the time τ_m it takes for the micelle to travel across the diffusive layer toward the surface. The exchange term $S_i(t)$ may then be ignored, and eq 2 can be solved for both unimers and micelles separately. It can now be written as:

$$\vec{v}\nabla\vec{c}_i = D_i\vec{\nabla}^2 c_i \quad (4a)$$

or

$$\alpha r z\frac{\partial c_i}{\partial r} - \alpha z^2\frac{\partial c_i}{\partial z} = D_i\left(\frac{\partial^2 c_i}{\partial r^2} + \frac{\partial c_i}{r\partial r} + \frac{\partial^2 c_i}{\partial z^2}\right) \quad (4b)$$

Close to the stagnation point we may neglect the variation in the r-direction and obtain:

$$-\alpha z^2\frac{\partial c_i}{\partial z} = D\frac{\partial^2 c_i}{\partial z^2} \quad (5)$$

On integrating this equation we find for $\partial c_i/\partial z$:

$$\frac{\partial c_i}{\partial z} = K_i\exp\left(\frac{-\alpha z^3}{3D_i}\right) = K_i\exp\left(\frac{-\bar{\alpha}Re\,\nu z^3}{3D_iR^3}\right) \quad (6)$$

where K_i is a constant, to be determined from the boundary condition that the total change in concentration between z = ∞ and $z = 0$ is given by the difference between bulk concentration c_i^b and the "subsurface concentration" of unadsorbed polymers c_i^s:

$$K_i = \frac{c_i^b - c_i^s}{\int_0^\infty \exp\left(\frac{-\alpha z^3}{3D_i}\right)dz} = p(c_i^b - c_i^s)\left(\frac{\alpha}{D_i}\right)^{1/3} \quad (7)$$

where the numerical constant p equals $9^{1/3}/\Gamma(1/3) \approx 0.776$. Here Γ denotes the gamma function.[21] The flux of polymer unimers and micelles toward the surface can now be written as

$$J_i = D_i\left(\frac{\partial c_i}{\partial z}\right)_{z=0} = D_iK_i = p(c_i^b - c_i^s)D_i^{2/3}\alpha^{1/3} = k_i(c_i^b - c_i^s) \quad (8a)$$

where the rate constant k_i is defined as

$$k_i = p\nu^{1/3}R^{-1}D_i^{2/3}(\bar{\alpha}Re)^{1/3} \quad (8b)$$

For uncharged polymers with affinity for the surface we may expect that the initial attachment rate is much higher than the transport rate k_i, i.e., every polymer chain that arrives at the surface will adsorb immediately. Thus, for the initial stage of the adsorption we may assume that c_i^s is zero and $d\Gamma_i/dt$ equals the limiting flux $J_i^{max} = k_ic_i^b$. On adsorption the surface is gradually filled with polymer and the attachment rate decreases. When the attachment rate becomes slower than the transport rate c_i^s will increase. Eventually, when the surface is completely occupied with polymer, c_i^s becomes equal to the bulk concentration. For a species that has no affinity for the surface, the attachment rate is zero and c_i^s equals the bulk concentration. For a micellar system with a relatively slow exchange rate, the total flux of polymer is simply given by the sum of the individual fluxes for unimers and micelles. When the corona of the micelles does not have affinity for the surface (but the hydrophobic block does), the

micelles cannot contribute to the flux and the total flux is equal to the flux of unimers.

Fast Exchange Rate

As the other extreme we assume that the exchange rate between unimers and micelles is relatively fast. The micelle breaks up into free polymers before it has reached the surface. At concentrations below the critical micelle concentration (cmc), the total flux of polymer is given by eq 8a for unimers. Above the cmc, however, the micelles that are present can be seen as a reservoir that instantaneously supplies new unimers until the cmc is reached again. This supply will continue up to a distance $z = \Delta$ from the surface, where the concentration of micelles drops to zero. From this point on the concentration of unimers decreases to become zero at the surface. We may now again take the source term $S_i(t)$ to be zero and solve eq 2 for unimers and micelles separately so that we again obtain eq 6 for $\partial c_i/\partial z$. However, the boundary conditions by which K_i is determined are different. For unimers, we have at the surface $c_u = c_u^s$, and at $z = \Delta$ the concentration is equal to c_u^b (the cmc). For the micelles, the concentration at $z \leq \Delta$ is zero, the concentration far away from the surface is equal to the bulk concentration, c_m^b. This leads to the following expressions for K_u and K_m.

$$K_u = \frac{c_u^b - c_u^s}{\int_\Delta^\infty \exp\left(\frac{-\alpha z^3}{3D_u}\right)dz} = \frac{(c_u^b - c_u^s)3\left(\frac{\alpha}{3D_u}\right)^{1/3}}{\Gamma'\left(\frac{1}{3}, 0, \frac{\alpha\Delta^3}{3D_u}\right)} \quad (9a)$$

$$K_m = \frac{c^b{}_m}{\int_\Delta^\infty \exp\left(\frac{-\alpha z^3}{3D_m}\right)dz} = \frac{3c_m^b\left(\frac{a}{3D_m}\right)^{1/3}}{\Gamma\left(\frac{1}{3}\right) - \Gamma'\left(\frac{1}{3}, 0, \frac{\alpha\Delta^3}{3D_m}\right)} \quad (9b)$$

Here Γ' is a generalized, incomplete gamma function.[21] The corresponding fluxes are obtained by multiplying $(\partial c/\partial z)_0$ and $(\partial c/\partial z)_\Delta$ with the diffusion coefficients D_u and D_m, respectively. An additional boundary condition is obtained from the conservation of mass: the flux of unimers at $z = \Delta - \partial z$ equals the flux of micelles at $z = \Delta + \partial z$, where ∂z is infinitesimally small.

$$D_u\left(\frac{\partial c_u}{\partial z}\right)_{z=\Delta} - D_m\left(\frac{\partial c_m}{\partial z}\right)_{z=\Delta} = K_u D_u \exp\left(\frac{-\alpha\Delta^3}{3D_u}\right) - K_m D_m \exp\left(\frac{-\alpha\Delta^3}{3D_m}\right) = 0 \quad (10)$$

Equations 9 and 10 can be solved numerically. We realize that the solution only gives a very rough description of the fluxes. Nevertheless, it can yield more insight in what occurs in real micellar systems. An impression of what will happen to the flux can already be obtained by taking a glance at eqs 9 and 10. In a solution of amphiphilic polymers the ratio between the total polymer concentration and the cmc is very important for the total flux of unimers toward the surface. When the total polymer concentration ($c_p = c_u + c_m$) in the bulk is equal to or lower than the cmc, no micelles are present, Δ is infinitely large, and K_m is zero. Consequently, eq 9a reduces to eq 7 for unimers. Keeping the polymer concentration c_p constant but decreasing the cmc will induce the formation of micelles, Δ becomes finite, and the flux of unimers at the surface is given by multiplying $(\partial c_u/\partial z)_0$ with the unimer diffusion coefficient D_u. Equation 9a has to be used for K_u. A further decrease of the cmc, while keeping c_p constant, will decrease Δ until this distance becomes infinitesimally small. With the help of eq 10 it can be seen that then $K_u D_u = K_m D_m$. In other words, for infinitesimally small cmc and Δ, eq 9b reduces to eq 7 for micelles, and the flux of *unimers* toward the surface can be approximately described by eq 8 for *micelles*. Summarizing these results for a micellar system with relatively fast exchange between unimers and micelles, when the total polymer concentration is kept constant and the cmc is decreased, the total polymer flux at the surface decreases from a value corresponding to that of a system without micelles ($K_u D_u$) to a value corresponding to the flux of micelles ($K_m D_m$).

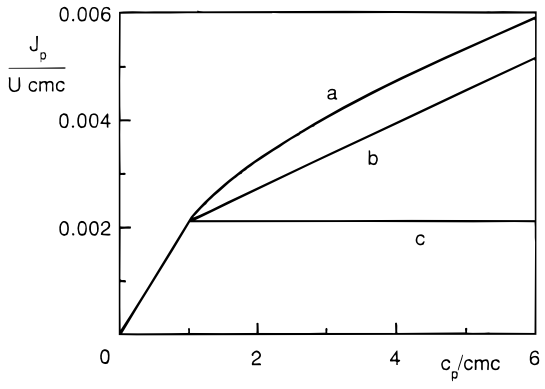

Figure 3. The flux of polymer toward the surface in a stagnation point flow as a function of the total polymer concentration. The flux and the concentration have been scaled by the mean velocity U and the cmc. Curve a was calculated with help of eqs 9 and 10 and assumes fast exchange between unimers and micelles; curve b, calculated with eq 8, is for a system without exchange and in which also the micelles adsorb, in curve c it is assumed that no exchange occurs and that micelles do not adsorb. For the diffusion coefficients we assumed $D_u = 10\ D_m$, and the streaming intensity parameter $\bar{\alpha}$ was taken as 2.

An experimentally more accessible quantity is the variation of the polymer concentration at constant cmc. For this situation we plotted in Figure 3 the flux of polymer toward the surface as a function of the total polymer concentration. The flux is scaled by the mean velocity U and the cmc. When the corona of the micelles is repelled by the surface and the exchange rate between micelles and unimers is very low, the flux is determined by the concentration of unimers solely, which results in a constant flux above the cmc (curve c). Even if micelles do not adsorb themselves, their presence can enhance the flux of unimers toward the surface considerably. If the exchange between micelles and unimers is fast, curve a is obtained. It is remarkable that this curve shows a higher flux than the sum of the individual fluxes of unimers and micelles (curve b). The adsorption kinetics of polymers forming nonadsorbing micelles with a fast exchange rate between micelles and solution, is thus faster than that of adsorbing micelles without exchange of unimers with the solution.

Whether the micelles and unimers can exchange or not depends on the relaxation time τ_r (which is inversely proportional to the exchange rate) and on the thickness of the micellar diffusive layer. The thickness of the diffusive or "stagnant" layer (δ_u) for unimers is given by the difference in concentration in the bulk and at z

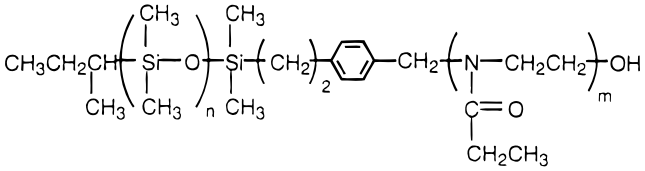

Figure 4. The structural formula of a PDMS−PEtOx diblock copolymer.

Table 1. Some of the Characteristics of the PDMS−PEtOx Diblock Copolymers[a]

sample code	wt % PDMS	M_n PDMS (kg mol^{-1})	M_n PEtOx (kg mol^{-1})	N PDMS	N PEtOx
0.5/2	17.2	0.5	2	7	20
2/8	17.0	2.2	10.7	29	108
5/20	19.8	4.8	19.6	65	198
20/80	15.2	20	80	270	808

[a] The first column gives the sample names in which the target molar mass for the blocks is indicated. The weight percentage PDMS was obtained from element analysis.[20] The number-average molar mass of samples 2/8 and 5/20 was determined by ^{29}Si NMR[29]; the molar masses of the othe samples were target values during synthesis. In the last two columns the degree of polymerization of the PDMS block and the PEtOx block are given, respectivley.

$= 0$, divided by the concentration gradient at the surface. For the diffusive layer thickness of the micelles (δ_m) we have to take the concentration and the concentration gradient at $z = \Delta$ instead of $z = 0$.

$$\delta_m = \frac{c_m^b - c_m^\Delta}{\left(\frac{dc_m}{dz}\right)_\Delta} \tag{11}$$

With this equation for the thickness of the diffusive layer we can calculate the time needed to diffuse across this layer, using the relation $\tau_m = \delta^2/2D_m$. If this time is much smaller than τ_r, the micelle will hardly supply new unimers. If τ_m is much larger than τ_r, most micelles will have broken up before they arrive at the surface, thereby enhancing the flux of adsorbing unimers toward the surface. Comparing the experimental initial adsorption rates of a range of polymers differing in chain length, and accordingly with different τ_m and τ_r values, gives us the opportunity to estimate the order of magnitude of the exchange rate constant.

Experimental Section

Materials. A series of four diblock copolymers of PDMS and PEtOx was used. The polymers were kindly given to us by Dr. J. S. Riffle, Virginia State University. The synthesis of these block copolymers proceeded by two steps, as described by Liu et al.[22] In the first step monofunctional PDMS oligomers were synthesized by living anionic ring-opening polymerization of hexamethyl trisiloxane and end functionalization with benzyl chloride endgroups. In the second step these oligomers were used to initiate the cationic ring-opening polymerization of 2-ethyl-2-oxazoline. The structural formula of the block copolymers is given in Figure 4, and some of the characteristics are given in Table 1. The refractive index increment of the block copolymers in solution must be known for reflectometry and is calculated from the values for the two different blocks, where we assumed the refractive index increment to be additive. For the poly(2-ethyl-2-oxazoline) block a value of 0.161 cm^3 g^{-1} was taken from ref 10. For the PDMS block we made a rough estimate by using $dn/dc = (n_p - n_s)/\rho_p$,[23] where n_p is the polymer refractive index (1.43),[24] n_s is the refractive index of the solvent (1.333), and ρ_p is the polymer density (970 kg m^{-3}, as determined with a low molar mass silicon oil). For the block copolymers this gives a rfractive index increment of 0.15 cm^3 g^{-1}. Polymer stock solutions of 10 g^{-1} in demineralized water were stored in the refrigerator.

Light Scattering

Dynamic light-scattering experiments were done with an ALV light-scattering apparatus (ALV, Langen, FRG) using a 400 mW argon ion laser tuned at a wavelength of 514 nm. All measurements were performed at $T =$ 297 K.

Transmission Electron Microscopy

Cryogenic temperature transmission electron microscopy (cryo-TEM)[25,26] was used to study the structure of the polymeric micelles in solution. These measurements were performed by Dr. P. M. Frederik and Mr. P. H. H. Bomans at the Department of Pathology of the State University of Limburg, The Netherlands. The polymer samples were prepared as follows. A copper TEM grid was dipped in a 10 g L^{-1} polymer solution. The aqueous solution was blotted away from the grid with a strip of filter paper, so that only a thin film of the sample spanned the holes. The grid then was plunged immediately into liquid ethane near its freezing point (T = 101 K). In this way, the thin water film containing micellar particles was vitrified. The sample was transferred under liquid nitrogen to a cryotransfer stage that was inserted into the TEM. Judging from published data it is very likely that the structures seen on the sample grid are the same as those present in the polymer solution.[27]

Reflectometry

The polymer adsorption measurements were performed with a reflectometer in an impinging jet flowcell as described in detail by Dijt et al.[28] For a stagnation point flow the transport of solute toward the adsorbing surface has been discussed by Dabros and Van de Ven.[20] In the preceding section we discussed the influence of the presence of micelles on the flux in the stagnation point. The flux can be described analytically by eq 8a. When the cmc is of the same order of magnitude as the polymer solution concentration c_p, the distance Δ must be calculated numerically from the experimental flux with eqs 9 and 10. For the calculations some experimental parameters must be known: in our experimental setup the viscosity $\nu = 10^{-6}$ m^2 s^{-1}, the dimensionless streaming intensity parameter $\bar{\alpha} = 2$, the Reynolds number $Re = 10.6$, and $R = 0.5$ mm. For the translational diffusion coefficients we used the values as measured by dynamic light scattering.

In a reflectometer[28] a polarized laser beam is reflected by the substrate in the cell. The substrate is a silicon wafer with a thin oxide layer. The reflected beam is split into its parallel and perpendicular components by a beam splitter; the respective intensities of these components, I_p and I_s, are detected separately and the signal S is calculated as $S = I_p/I_s = f\,R_p/R_s$, where f is an apparatus constant that can be found by calibration, and R_p and R_s are the reflectivities of the parallel and the perpendicular components. Upon adsorption a thin polymer layer is formed with a refractive index differing from that of the substrate and the solution. The signal changes by an amount ΔS, and the relative change $\Delta S/S_0$ is proportional to the adsorbed amount Γ.

Macroscopically flat silicon wafers with a refractive index $n = 3.8$ from Aurel GmbH (Germany) were used. With these as the starting material, we prepared both

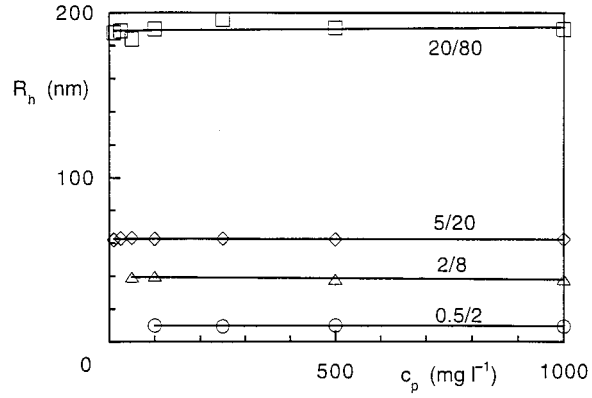

Figure 5. The hydrodynamic radius of four PDMS−PEtOx diblock copolymers in an aqueous solution as a function of the polymer concentration as measured by dynamic light scattering at a scattering angle of 90°.

silica- and titania-coated wafers. Silica layers were prepared by thermal oxidation in dry air. This gives a SiO_2 layer with a thickness of about 110 nm and $n = 1.46$. TiO_2 layers with a thickness of about 25 nm and $n = 2.33$ were deposited by reactive sputtering of Ti in an oxygen atmosphere. This was carried out at Philips Laboratories in Eindhoven, The Netherlands. Strips cut from these wafers were cleaned by oxidation with UV-ozone, and could be cleaned and reused many times.

Results and Discussion

Block Copolymer Solutions. Dynamic Light Scattering. The block copolymers of PDMS−PEtOx are amphiphilic with a hydrophobic PDMS block and a hydrophilic PEtOx block. In an aqueous solution we therefore expect these polymers to form micellar structures. Indeed Nagpal et al.[29] found micelles in solution for two of these block copolymers. As in their article, we also used dynamic light scattering to measure the size of these micelles. In Figure 5 we plotted the micellar hydrodynamic radius (R_h) as a function of polymer concentration for the four polymer samples, measured at a scattering angle of 90°. In the data analysis we used the cumulant method described by Koppel.[30] The hydrodynamic radius of the micelles was calculated with the Stokes−Einstein relation for spherical particles. This may not be entirely correct for nonspherical micelles. Nevertheless, it gives a good impression of the size of these scattering particles.

The measured hydrodynamic radius and the scattered intensity were constant for at least two weeks after preparation of the polymer solutions, indicating that the polymers in these solutions are very likely to have their equilibrium conformation. The average hydrodynamic radius of the PDMS−PEtOx polymer micelles is 10, 39, 63, and 190 nm for 0.5/2, 2/8, 5/20, and 20/80, respectively, and does not change with the polymer concentration. Nagpal et al.[29] found an average hydrodynamic radius of 81 nm for 2/8 (in their paper denoted as PETOX-PDMS 11k-2k). This large value was attributed to the aggregation of relatively small micelles caused by the association of the PEtOx chains in the coronas. We found a smaller radius, 39 nm, for 2/8 and the particles were rather polydisperse as indicated by a considerable increase of the measured radius at a low scattering angle. For 5/20 Nagpal et al.[29] found an average hydrodynamic radius of 15 nm, considerably lower than the value of 62 nm measured by us. From the very small increase in radius at low scattering angle they concluded that this block copolymer forms rather compact micelles with a narrow size distribution. Again, our sample showed a considerable increase in hydrodynamic radius at decreasing scattering angle, indicating a broad size distribution. The radius reported by Nagpal et al. for compact micelles of 5/20 was 15 nm, which is even smaller than our result for 2/8, which has a lower molar mass. This also indicates that, although the size we found for 2/8 is smaller than reported by Nagpal et al., we probably have larger structures than that of compact single micelles. Also for the PDMS−PEtOx samples 0.5/2 and 20/80 we found a rather broad size distribution.

To find out whether there are two populations in the solution, compact single micelles and aggregates of micelles, we also performed a constrained regularization analysis[31,32] on the light scattering data (with the regularized continuous inversion algorithm CONTIN). With this method a bimodal distribution can be revealed. However, this analysis showed only one peak at about the same radius as found by the cumulant analysis. Thus the solution contains only one population of rather polydisperse micelles. We cannot exclude the possibility that compact micelles are slightly aggregated in larger structures. However, it is also possible that the micelles have a nonspherical structure and are very polydisperse.

Transmission Electron Microscopy. The structure of the micelles in solution was investigated with cryo-TEM. The process of sample vitrification is very fast (10 μs) which makes it very likely that the structures in the aqueous solution are kept in their original state. In Figure 6 we show the TEM pictures of 10 g L^{-1} aqueous PDMS−PEtOx diblock copolymer solutions of 2/8 (a), 5/20 (b), and 20/80 (c). For 0.5/2 the picture did not show any structure, indicating that particles are either absent or too small to be detected by cryo-TEM (i.e., the radius is smaller than a few nanometers). The density of PEtOx chains in the solubilized corona of the micelles is relatively low, making it unlikely that this corona can be seen on the TEM pictures.[33,34] The structures we see are therefore mainly the parts containing predominantly hydrophobic PDMS. In Figure 6a we see for 2/8 more or less spherical structures with a radius between 8 and 16 nm; the size distribution of the structures is rather broad. Polymer 5/20 gives spherical structures with a radius varying from 12 to 20 nm (Figure 6b). In Figure 6c we see that 20/80 forms oval structures with radii varying from 20 to 40 nm; however, long rods with a thickness of 30 nm also are present. We see clusters of compact micelles for none of the samples. The structures are smooth and do not show dark spots, which could be attributed to the existence of such small and compact micelles within one aggregate. The total size of the PDMS−PEtOx micelles is rather large if we consider that the contribution of the PEtOx chains is not seen.

The size as measured by dynamic light scattering is much larger than found by TEM. This is partly because TEM does not show the corona of the micelles. Also very important is the polydispersity of the structures seen by TEM. In light scattering the contribution of large structures is generally much greater than that of small objects. The existence of a few large structures can increase the measured average hydrodynamic radius considerably. For 20/80 we even find rods in solution.

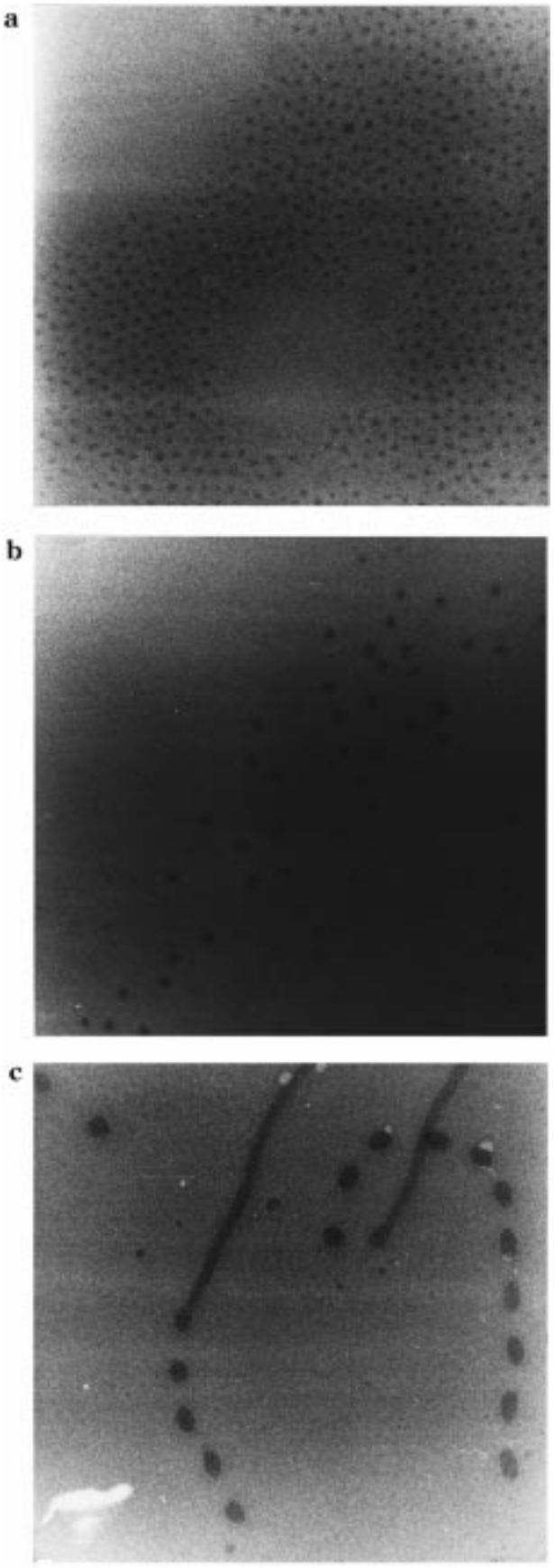

Figure 6. Cryotransmission electron micrograph pictures of 10 g L^{-1} aqueous PDMS−PEtOx diblock copolymer solutions of 2/8 (a), 5/20 (b), and 20/80 (c).

These long rods have a low diffusion coefficient and increase the radius as measured by dynamic light

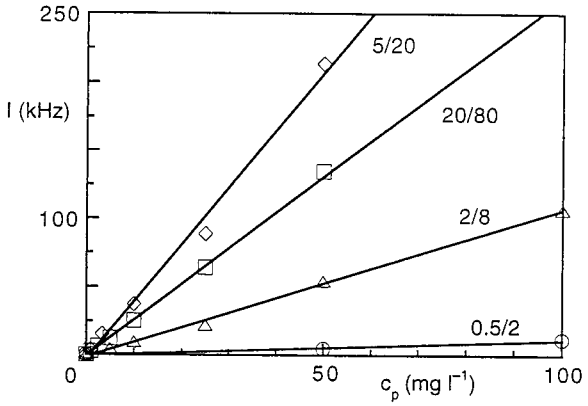

Figure 7. The scattered intensity of PDMS−PEtOx diblock copolymers in an aqueous solution as a function of the polymer concentration measured by dynamic light scattering at a scattering angle of 90°.

scattering substantially. The large structures may arise because water is not a very good solvent for PEtOx; the solution shows an LCST at 329 K, and the solvency parameter χ at room temperature is 0.48,[35,36] which is rather close to phase-separation conditions.

Scattered intensity: The cmc of the block copolymer solutions in principle can be determined from a plot of the scattered light intensity as a function of the polymer concentration. This plot should have a linear part, the intersection of which with the concentration axis is at the cmc. Such a plot is given in Figure 7 for all polymer samples at a scattering angle of 90°.

The scattered intensity of the solution with the smallest polymer (0.5/2) is low and the lowest concentration at which we could do reliable measurements was 50 mg L^{-1}. For 2/8 the lowest concentration was 5 mg L^{-1}. For the two block copolymer samples with the highest molar mass (5/20 and 20/80) the lowest concentration was 1 mg L^{-1}. It can be seen that the intensity is a linear function of the polymer concentration for all polymers used. The intersection with the concentration-axis, which gives the cmc, is, within experimental error, at zero polymer concentration. The cmc of these polymer solutions is thus lower than the lowest concentration that gave reliable values: 50, 5, 1, and 1 mg L^{-1} for 0.5/2, 2/8, 5/20, and 20/80, respectively. Liu et al.[22] measured the surface tension of a solution of 0.5/2 as a function of the concentration. From these measurements they obtained a cmc value of approximately 70 mg L^{-1}. This value is higher than the upper limit of the cmc from our light scattering data. For polymer solutions the determination of the cmc from surface tension measurements is problematic. Because the diffusion coefficient of polymers is much lower than that of low molar mass surfactants, the time needed to obtain equilibrium can be rather large, so that equilibrium between the solution and the surface is not guaranteed. For light scattering, equilibrium with the surface is not required. Also, it is not a problem to wait a long time before doing the measurements.

It is remarkable that the scattered intensity of 5/20 is higher than that of a 20/80 solution. Just the reverse was expected, because the scattered intensity is a function of the size of the scattering particle. The form factor of the micelles was not responsible for this result, because we did not find minima and maxima as a function of the scattered angle, which is probably due to the polydispersity of the micelles. However, the

scattered intensity at a certain angle is a complicated quantity in which not only the radius of the particles but also the difference between the refractive index of the scattering particle and that of the solvent plays an important role.[37] Increasing the difference between the refractive indices will increase the scattered intensity. The radius of 20/80 is three times larger than the radius of 5/20; nevertheless, the scattered intensity is lower. This may be explained by the more compact micelles of 5/20 molecules compared with the aggregates formed by 20/80. The latter forms both oval particles and rodlike structures, as seen from the TEM-picture in Figure 6c. The rods decrease the diffusion coefficient (and hence increase the Stokes radius derived from it) but, on the other hand, decrease the average polymer density which presumably reduces the average refractive index. As a result, the scattered intensity could be relatively low, even when the hydrodynamic radius is rather large.

Adsorption. As we saw in the preceding section, the diblock copolymers used in this study form micellar structures in an aqueous solution. The corona of the micelles is formed by PEtOx chains, whereas the core consists of PDMS, which forms a melt of flexible chains because the glass-transition temperature of PDMS (T_g = 146 K)[24] is well below room temperature. The micelles are rather large polydisperse structures. Before we turn to the adsorption of the block copolymers, we first investigate the behavior of both homopolymers at a silica and a titania surface.

From a previous study[10] and from literature[35] we know that the homopolymer PEtOx adsorbs onto silica. We found an adsorbed amount of 0.58 mg m^{-2} for a molar mass of 6000. In the present work we also considered the system PEtOx/titania, but we did not observe any adsorption in this case. The hydrophobic PDMS is reported to have affinity for silica,[38] but for its interaction with titania we could not find any results in the literature.

For the micelles formed by block copolymers of PDMS−PEtOx this means that in silica both the PEtOx corona and the PDMS core have surface affinity. This will cause a competition between PEtOx and PDMS for surface sites. In equilibrium the block with the highest adsorption energy will displace the other one. For these amphiphilic polymers the hydrophobicity of the PDMS block is an extra driving force that favors the adsorption of PDMS. For the polymer/silica system it therefore seems most likely that in the equilibrium situation the PDMS block will adsorb and the PEtOx block will remain in solution. In titania the PEtOx corona does not have affinity for the surface. When the PDMS has affinity, the equilibrium adsorbed state will be similar to that on silica: an adsorbed block copolymer layer with a molten layer of PDMS in contact with the surface and PEtOx blocks protruding into the solution. Because PEtOx adsorbs on silica but not on titania, we envisage different scenarios for the build-up of the adsorbed layer on either surface. Measurements of the kinetics of adsorption can tell us which scenario is adequate and provide information about the adsorption mechanism of amphiphilic block copolymers.

Adsorption Curves of the Block Copolymers: We measured the adsorbed amount as a function of time for all four PDMS−PEtOx diblock copolymer samples onto silica and titania with reflectometry. The adsorption curves for 0.5/2 on silica and titania are given in Figures 8a and 8b, for 2/8 in Figures 8c and 8d, for 5/20 in Figures 8e and 8f, and for 20/80 in Figures 8g and 8h, respectively.

To discuss the different features of the adsorption curves, we first look at Figure 8g for 20/80 onto silica. Several different regimes can be distinguished in one adsorption curve. In the first part of the curve the adsorption increases rapidly and linearly with time until an adsorbed amount of around 0.6 mg m^{-2} is reached (regime a). The slope of the adsorption curve then decreases rather abruptly to a new value. In this second regime (regime b) the adsorbed amount increases again more or less linearly with time up to a very high adsorbed amount, where we find a third regime (regime c) with a decreasing slope until a *plateau* is reached.

Figure 8h shows the corresponding adsorption curve on titania. The shape of this curve is different from that found on silica. The adsorption increases approximately linearly up to a rather high adsorbed amount (regime b), after which the slope decreases (regime c), and finally a *plateau* is reached. It is remarkable that the initial adsorption rate on titania is, on first approximation, equal to the adsorption rate in regime b on silica. This first regime on titania is therefore denoted regime b. Regime a, which was found on silica, is entirely missing on titania.

In Figure 9 we enlarged the first stages of the adsorption curves of all four diblock copolymers on silica, emphasizing regime a and (the beginning of) regime b. For all samples, the constant adsorption rate in regime a is the same up to an adsorbed amount between 0.2 (for 0.5/2) and 0.6 mg m^{-2} (for 20/80). There is a fairly sharp transition to regime b. The drop in adsorption rate from (regime a) to (regime b) is most pronounced for the diblock copolymer with the highest molar mass.

As is seen from Figures 8 and 9 the shape of the adsorption curves differs for the four polymer samples and depends also on the substrate. For 0.5/2 on silica we see that regime b lies between 0.4 and 3.0 mg m^{-2}. The adsorption rate then decreases rather abruptly in a narrow regime c; at the plateau of the curve the adsorbed amount is constant at 3.5 mg m^{-2}. On titania, regime b extends up to an adsorbed amount of approximately 1.0 mg m^{-2}. From this point, the adsorption rate decreases slowly, i.e., regime c is very wide. In the plateau the adsorbed amount is considerably lower than on silica (1.7 mg m^{-2}).

The shape of the adsorption curves of 2/8 is more rounded, the linear regimes are short, and in most parts of the curve, the adsorption rate is decreasing. This could be an indication that the polymers or the micelles are very polydisperse. The adsorbed amounts are higher than found for the short chains. The difference between the adsorbed amounts in the plateau on silica and titania is small: 4.9 and 4.2 mg m^{-2}, respectively.

The adsorption curve of 5/20 shows an extremely long regime b. On silica, the adsorption rate is constant up to an adsorbed amount of 6 mg m^{-2}. In regime c the adsorption rate decreases smoothly, and the plateau is approximately 8.5 mg m^{-2}. On titania, the adsorption increases linearly up to about 4 mg m^{-2}, and the adsorbed amount in the plateau of the curve is 6.3 mg m^{-2}.

The shape of the adsorption curves of 20/80 on silica and titania is slightly rounded. Regime b extends up to approximately 3 mg m^{-2} for both silica and titania. The decrease of the adsorption rate in regime c is rather slow and the plateau value is reached only after a very long

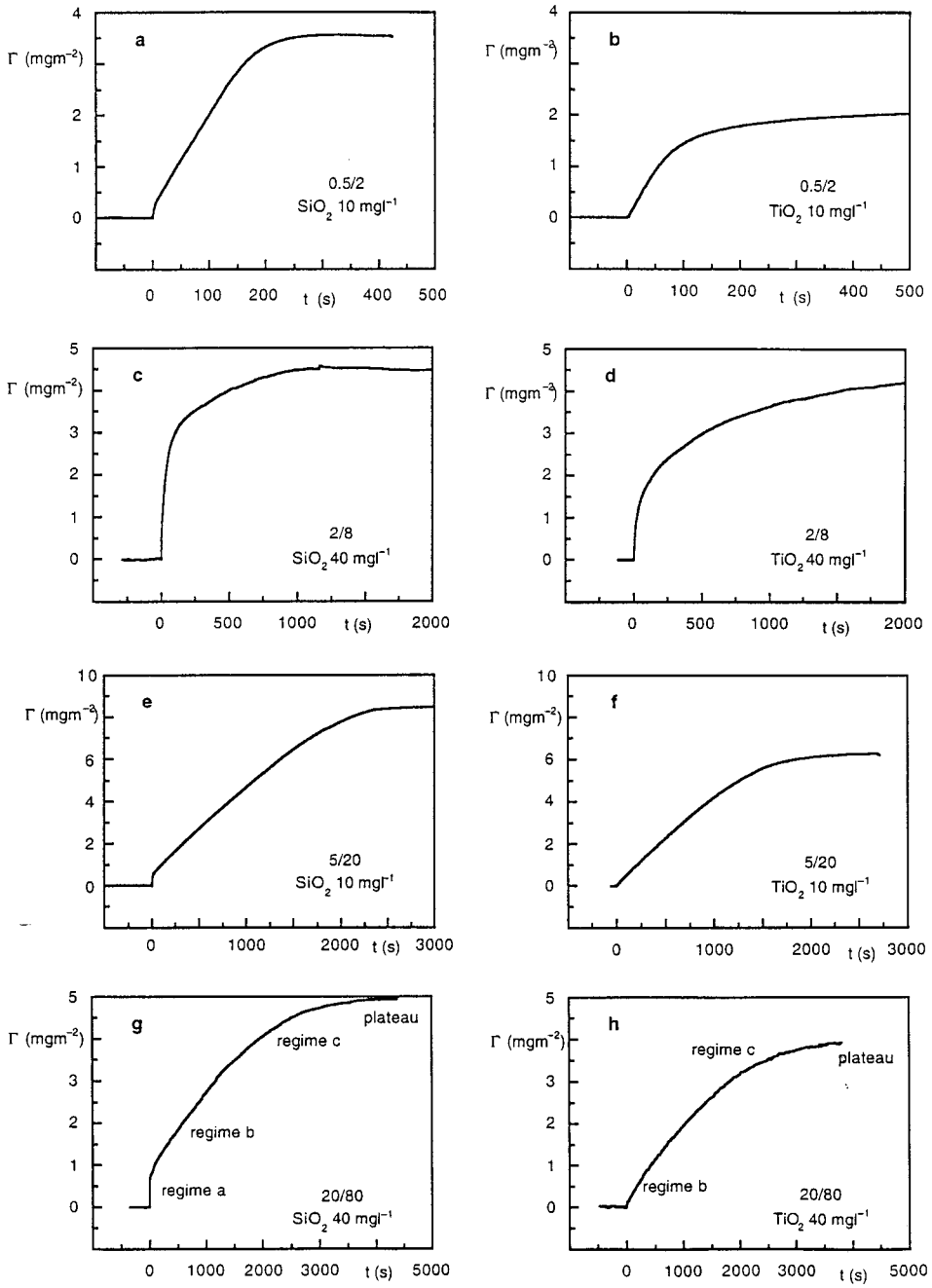

Figure 8. The adsorption of PDMS−PEtOx block copolymers onto SiO_2 and TiO_2 from aqueous solution as a function of time. The polymer concentration was 10 or 40 mg L^{-1} and is indicated in the plot. The results for 0.5/2 on silica and titania are given in plots a and b, respectively, for 2/8 in plots c and d, for 5/20 in plots e and f, and for 20/80 in plots g and h. The meaning of the different regimes shown in plots g and h is given in the text.

adsorption time, or with the use of a high polymer concentration. The adsorbed amounts in the plateau are approximately 5.0 mg m^{-2} on silica and 3.7 mg m^{-2} on titania, respectively. The adsorbed amounts in the plateau of the adsorption curves on silica and titania for each of the polymers are collected in Table 2.

Regime a: The adsorption rate in regime a for 20/80 is plotted in Figure 10 as a function of the polymer concentration in solution. It is clear that the initial adsorption rate increases linearly with concentration. The slope of the initial adsorption rate as a function of concentration (the rate constant) is 6.0×10^{-6} m s^{-1}. Also for the other block copolymers we found that the initial adsorption rate increased linearly with the polymer concentration; the adsorption rate appeared to be approximately equal for all samples (between 6.0 and 7.3×10^{-6} m s^{-1}).

A first attempt at interpretation is to ascribe the initial part of the adsorption curve on silica to the adsorption of micelles with a PEtOx corona that has affinity for the surface. This also would explain the absence of this regime in the adsorption curve on titania, because the PEtOx chains in the corona have no affinity for titania. We would then expect the initial rate to depend on the diffusion coefficient of the micelles. However, we do not find such a relation. Another argument against the adsorption of micelles in the initial part was obtained when we filtered the solution of the largest diblock copolymer 20/80 through an 0.22-μm Millipore filter. Large micelles were no longer

Table 2. The Adsorption Rate Constants in Regime b of the Adsorption Curves on Silica and Titania for the PDMS−PEOx Diblock Copolymers[a]

sample PDMS−PEtOx	$d\Gamma/dt/c_p$ regime b SiO_2 (10^{-6} m s^{-1})	$d\Gamma/dt/c_p$ regime b SiO_2 (10^{-6} m s^{-1})	J_m/c_p (10^{-6} m s^{-1})	Γ_{pl} SiO_2 (mg m^{-2})	Γ_{pl} TiO_2 (mg m^{-2})	δ_m (10^{-6} m)	τ_m (s)
0.5/2	1.75	1.82	3.62	3.5	1.7	6.6	0.9
2/8	1.53	1.70	1.46	4.9	4.2	4.2	1.4
5/20	0.40	0.45	1.06	8.5	6.3	3.5	1.7
20/80	0.038	0.056	0.508	5.0	3.7	2.5	2.4

[a] In the fourth column the theoretical flux of micelles toward the surface is given, as calculated with eq 8. We assume that the total polymer concentration and the micelle concentration are equal (i.e., cmc is very small) and used the diffusion coefficient as measured by dynamic light scattering. The fifth and the sixth columns show the plateau adsorbed amounts. In the last two columns the micellar diffusive layer thickness δ_m and the time τ_m a micelle needs to diffuse across this layer are given. All measurements were done in an aqueous solution with a pH between 5 and 6 and a temperature of 295 K. The polymer concentrations were varied between 2 and 50 mg L^{-1}.

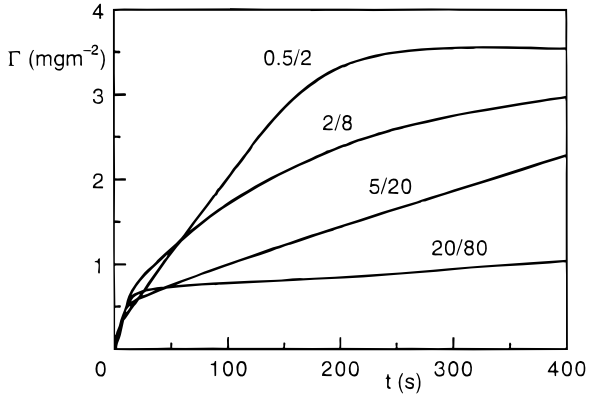

Figure 9. The first stages of the adsorption curves of four PDMS−PEtOx block copolymers onto silica as measured with reflectometry. The concentration of 0.5/2 and 5/20 was 10 mg L^{-1}, for 2/8 and 20/80 the measurements were done at 40 mg L^{-1} but the curves were rescaled to a polymer concentration of 10 mg L^{-1}.

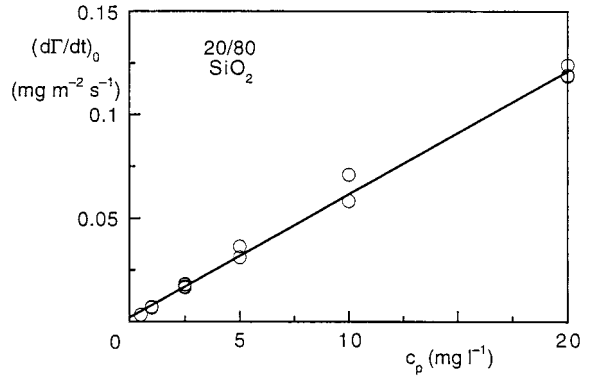

Figure 10. The initial adsorption rate $(d\Gamma/dt)_0$ on silica (in regime a) as a function of the polymer concentration for 20/80. The linear fit has a slope of 6.0×10^{-6} m s^{-1}.

present. However, when we measured the adsorption of this sample onto silica, we found an adsorption curve with the same initial adsorption rate as for the unfiltered solutions. However, the adsorbed amount in the plateau was only 0.7 mg m^{-2}. This indicates that something other than micelles adsorbs in the initial part of the adsorption curve on silica. Because the cmc is very low, it is most probable that there is some contamination in our samples that adsorbs on silica and not on titania. If the contamination is a low-molar-mass material, low concentrations already give a considerable flux toward the surface, similar to the adsorption rate measured in regime a. We have not been able to determine the exact chemical nature of the contamination, but it seems likely that it is oligomers of EtOx formed during the cationic polymerization of ethyl oxazoline. These short fragments will be displaced easily by the block copolymers, so that their presence is of little consequence for the block copolymer adsorption process.

Regime b: Regime b in the adsorption curves on silica and on titania is linear in the polymer concentration. As seen in Figures 8 and 9, the adsorption rate in this regime depends on the type of polymer. For 20/80 this adsorption rate is extremely low. We plot this rate as a function of polymer concentration in Figures 11a and 11b for silica and titania, respectively. Because the adsorption rate for this polymer is very low, its determination is somewhat inaccurate. For the smallest polymer, 0.5/2, the rate is much higher, and these results are given in Figures 11c and 11d. Within experimental error the same slope is found for regime b on both surfaces. From Figure 11 we determined the adsorption rate constants in regime b for 0.5/2 and 20/80. For the other two polymer samples the rate constants were obtained in a similar way. The results are given in Table 2. For comparison we also included the theoretical flux as calculated for micelles with eq 8a, assuming that only micelles exist in solution (which is approximately correct when the cmc is low). In the same table we also give the adsorbed amounts in the final plateau.

Adsorption on Titania: Some interesting conclusions can be drawn from the adsorption kinetics. The adsorption from micellar solutions of the block copolymers onto titania, for which surface the corona has no affinity, most likely proceeds by the adsorption of free unimers.[7] The adsorption experiments were all performed well above the cmc, with the possible exception of the smallest polymer, for which the concentration may be of the order of the cmc. If the exchange rate between micelles and unimers is relatively slow, we expect the initial adsorption rate in regime b to be very low. The rate would then be determined by the cmc and would not vary with the total polymer concentration. However, we see in Figures 11b and 11d that the adsorption rates depend linearly on the concentration for all polymer samples. This result must be attributed to the presence of micelles, which supply new unimers, thereby contributing to the adsorption rate. Thus, the exchange of free unimers between micelles and solution must be taken into account.

When we look at Figure 3, which gives the theoretical flux of polymer toward the surface, we see that an inflection point is found at the cmc. The experimental results for titania in Figure 11 do not show such an inflection point, indicating that all polymer concentrations were indeed above the cmc and that the cmc of all

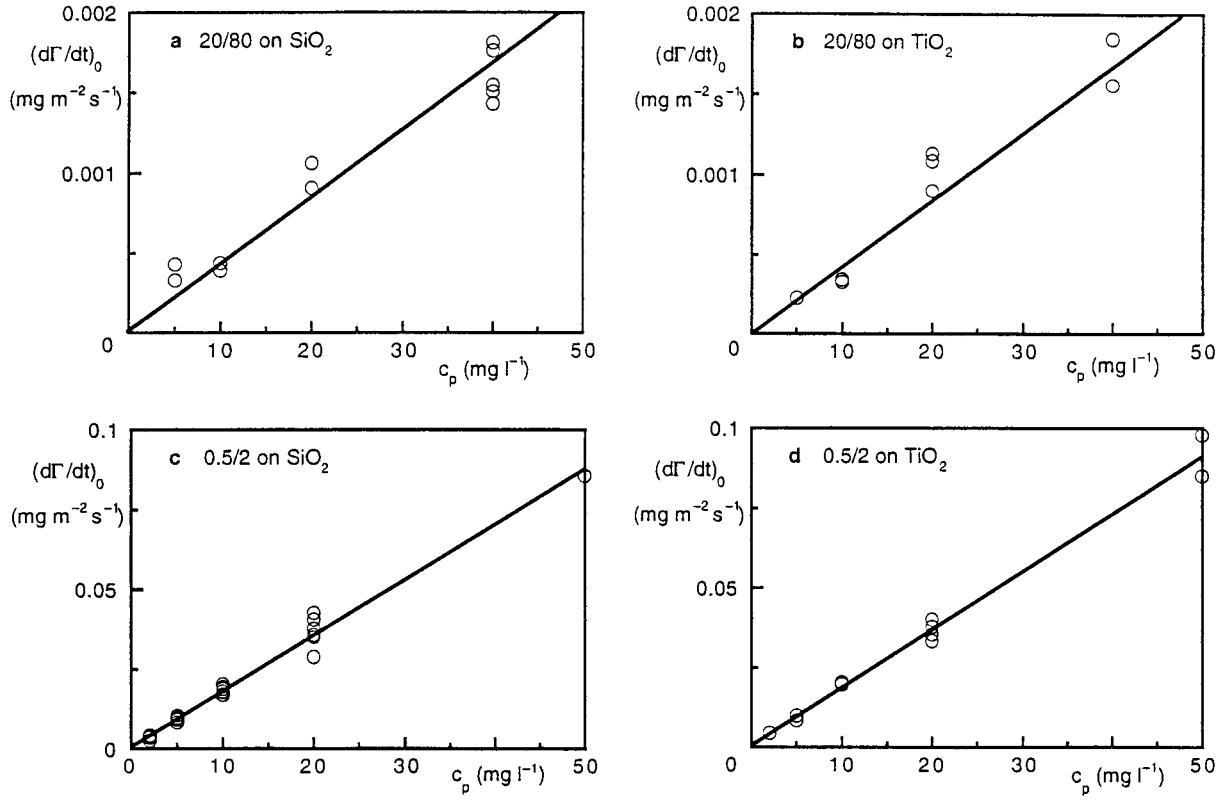

Figure 11. The adsorption rate in regime b for the largest polymer (20/80) and the smallest polymer (0.5/2) on both silica and titania as a function of the polymer concentration.

four polymer samples is below 2 mg L^{-1}. For the three largest polymers this was already known from the dynamic light scattering data, but for the smallest polymer 2 mg L^{-1} is considerably lower than the upper limit that we determined from our light scattering data.

For a relatively fast exchange of unimers between micelles and solution, we can describe the flux of polymer toward the surface with eq 8a for micelles (curve b in Figure 3). When we compare the experimental adsorption rate constants on titania with the theoretical rate constant for the flux of micelles toward the surface, we see that the experimental value for 20/80 is about 10 times lower than the calculated flux of micelles. For polymers 0.5/2 and 5/20 the value is about half the theoretical flux, and for polymer 2/8 the experimental value is close to the theoretical flux. However, this polymer showed a rather rounded adsorption curve, which indicates that the sample is rather polydisperse. Therefore, the experimental flux is likely to be dominated by the small micelles, whereas the theoretical flux is calculated from the average diffusion coefficient as measured by dynamic light scattering, where large micelles are relatively more important. We realize that the values of the theoretical and experimental fluxes are not really quantitative. Roughly speaking, we can state that the experimental flux of the three smallest polymers is similar to the theoretical flux, whereas the experimental flux of the largest polymer is an order of magnitude lower than the theoretical flux. Thus, the exchange of unimers between micelles and solution must be relatively fast for the three polymers with the lowest molar mass, whereas for 20/80 the exchange is slower than the time needed to diffuse across the diffusive layer. Most micelles arrive at the surface before they have fallen apart, and, because the corona does not have affinity for the titania surface, they will not contribute to the adsorption.

Micellar Relaxation Time: The thickness of the micellar diffusive layer δ_m can be calculated from eq 11b. For a concentration much higher than the cmc, Δ approaches zero, and δ_m can be calculated easily. In Table 2 the thickness of the micellar diffusive layer for all polymer systems has been included. The thickness is between 2.5 μm for the large micelles of 20/80 and 6.6 μm for the small micelles of 0.5/2. From these values and the relation $\tau_m = \delta_m^2/2D_m$, it is now possible to estimate the average time τ_m a micelle needs to diffuse across this layer. This time has also been included in Table 2. The micellar relaxation time (τ_r) is the time a micelle needs to break up in free polymers. The three smallest polymers have a micellar relaxation time τ_r that is smaller than τ_m, because these micelles break up before they arrive at the surface. The largest polymer has a micelle relaxation time τ_r that is larger than the micellar diffusion time τ_m; we estimate that it is a few tens of seconds. The high relaxation time for the large micelles of 20/80 can be explained by the high molar mass of this polymer. The hydrophobic block has to diffuse out of the core into a nonfavorable environment and to travel through the corona before it can enter the solution. By increasing the molar mass the barrier becomes higher due to the larger hydrophobic block for which the chance to "escape" is much lower. Because the molar mass of the largest polymer is 40 times higher than that of the smallest polymer, the micellar relaxation will be several orders of magnitude slower.[19] The time to diffuse across the diffusive layer depends also on the molar mass, but this dependence is much weaker. Plots of τ_m and τ_r as a function of molar mass would probably intersect for the polymers in this study.

Another factor contributing to the barrier is the viscosity of the micellar core. In our system the core is a true melt of flexible PDMS. Many stiffer hydrophobic polymers form a glassy core in which the polymer motion is frozen. The exchange of free polymers between micelles and solution will then be extremely slow and equilibrium may not be attained. By changing the solvent conditions one can plasticize such a glassy core. The effect of solvent has been studied by Dewalt et al.[39] for polystyrene−poly(ethylene oxide) block copolymer adsorption onto polystyrene particles from an aqueous solution. In pure water they did not observe adsorption but by adding some tetrahydrofuran (THF), a good solvent for the PS polystyrene (PS) core, they found that adsorption did occur. In the glassy state the adsorption from the micelles was probably kinetically blocked.

Adsorption on Silica: For the silica surface the corona of the micelles can also attach to the surface. However, as we have seen from the results on titania, the micelles of the three smallest polymers will have broken up into unimers before they arrive at the surface. Hence, for the three smallest polymers the adsorption on silica also proceeds by the attachment of unimers. For the largest polymer the exchange of unimers between micelles and surface is not fast enough, and part of the micelles will be able to reach the surface. These intact micelles can adsorb with their corona and the polymer could form a mixed layer of adsorbed unimers and micelles. One would then expect that the adsorption rate equals the theoretical flux of micelles toward the surface. The adsorption rate in regime b for 20/80 on silica would then be different from that found on titania. However, from Table 2 we see that this does not hold: the experimental rate on silica is much slower than the theoretical flux of micelles and equals that of titania. Apparently, the corona is inhibited from adsorbing to the surface. A possible explanation is the existence of the contamination in the polymer sample, as mentioned before. This contamination gives rise to regime a and probably forms a thin layer that inhibits the adsorption of the PEtOx corona. The hydrophobic block of the unimers has a very high affinity for the surface and can displace the layer of contaminant molecules. Consequently, the adsorption rate, as for the adsorption on titania, is governed by the exchange rate between micelles and unimers.

Adsorbed Amount: The plateau adsorbed amount on silica is higher than on titania. This is an indication that the PDMS block has a higher affinity for silica than for titania. The adsorption curves on titania are more rounded than on silica, and especially regime c is longer. In this regime a barrier is formed by the brush of PEtOx chains. Although the lateral pressure in this brush may not be very high, because water is almost a theta solvent for the PEtOx chains, the brush could reduce the kinetics of adsorption considerably. However, the adsorbed amount on silica is higher than on titania, implying that the brush is denser and has a higher lateral pressure. We would then expect that regime c is wider for silica than for titania. Because this is not the case, the adsorption kinetics is more likely to be governed by the adsorption energy at the surface, rather than by the steric barrier of the brush.

The plateau adsorbed amounts are much higher than usually found for homopolymers. The presence of a long, nonadsorbing block, combined with a strongly anchoring block, gives rise to a real anchor-buoy structure with a high adsorbed amount, which is typical for diblock copolymer adsorption. For a constant composition, the adsorbed amount is expected to increase with the total length of the block copolymer.[3,5] This trend is followed for the three polymers with the lowest molar mass, but the plateau adsorbed amount for the largest polymer 20/80 is considerably lower than for sample 5/20. The maximum adsorbed amount probably is not yet reached for the longest polymer. The barrier formed by the PEtOx chains of adsorbed molecules in this case extends over a very long distance. Although the density of this brush is less than for the brush of the smaller polymer, the long distance over which unimers have to diffuse constitutes an enormous kinetic barrier. Therefore, it can take a very long time before equilibrium is obtained. Reflectometry is not suitable to measure on time scales more than a few hours, so that another technique should be used to study the equilibrium state for such long polymers.

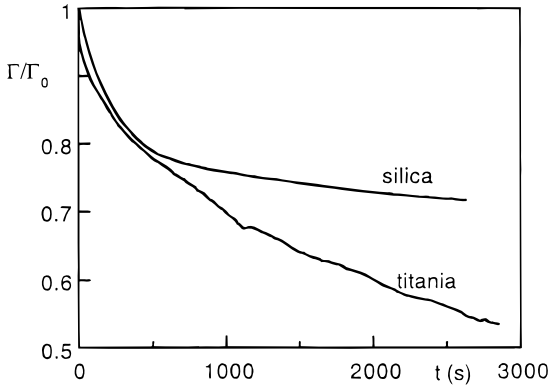

Figure 12. Desorption of 0.5/2 upon dilution with water from silica and titania.

Desorption. Desorption of the polymers upon dilution by pure solvent was also studied. The desorption was negligible for the three polymers with the highest molar mass. However, the desorption of 0.5/2 was rather large. In Figure 12 we plotted the desorption of this polymer upon dilution on silica and on titania. The adsorbed amount is scaled to the adsorbed amount at the plateau, the time-axis runs from the onset of desorption.

The desorption on silica and titania is relatively fast until about 20% of the material has desorbed; from that point on, the desorption behavior on both surfaces is different. On titania the desorption continues, although the desorption rate gradually decreases. On silica the desorption rate declines rapidly, and the adsorbed amount becomes almost constant. Nevertheless, even after 40 min polymers still desorb from both surfaces. The desorption from silica has roughly a log t dependence, whereas the desorption from titania seems to be faster than logarithmically. The fact that the desorption rate on titania is higher than on silica points to a stronger interaction of the polymer with silica. This interaction must be attributed to the hydrophobic block; in the saturated layer the hydrophilic blocks are not in contact with the surface. This conclusion is in agreement with the lower adsorbed amounts on titania, from which we already deduced that the adsorption energy on silica is higher than on titania.

The behavior of the diblock copolymer 0.5/2 is similar to that of a surfactant. Because of the small number of segments surfactant molecules can be desorbed easily upon dilution.[40] The hydrophobic PDMS block contains

only seven siloxane segments, and the hydrophilic PEtOx block consists of 20 segments. This is more than for most common surfactants, but this sample is not really polymeric either. The intermediate behavior between that of a small surfactant and a long polymer gives a very slow desorption of the molecule upon dilution.

Conclusions

In this article the solution and adsorption behavior of amphiphilic diblock copolymers was considered. Four diblock copolymers of hydrophobic PDMS and hydrophilic PEtOx were studied. The block copolymers only differed in their total molar mass; the ratio PEtOx/PDMS was approximately constant (block length ratio between 5 and 6). In an aqueous solution these block copolymers formed large polydisperse micelles. For the polymer with the highest molar mass we found oval micelles and rods in the solution, as revealed with cryo-TEM. The cmc could not be determined but was lower than 2 mg L^{-1}.

Both blocks of the copolymers have affinity for silica, and only the hydrophobic block has affinity for the titania surface. The adsorption of these polymers onto macroscopically flat oxide surfaces was studied with reflectometry in a stagnation point flow cell. We were able to follow the time-dependent adsorption up to several hours after the onset of adsorption. Apart from a small contribution of a low-molar-mass contaminant to the curve on silica, the adsorption curves on silica and titania show similar features. The contaminant prevents the corona of the micelles from adsorbing onto silica, so that on both surfaces the adsorption behavior is governed by the adsorption of the hydrophobic blocks The adsorption kinetics is clearly affected by the exchange rate between micelles and free polymers. For the three smallest molar masses the exchange rate is fast compared with the time a micelle needs to diffuse across the diffusive layer. Before the micelles arrive at the surface they have already broken up into free polymers. Because the cmc is very low, the experimental adsorption rate is determined by the diffusion of micelles toward the surface. For the longest polymer this is not the case: the exchange of unimers between micelles and solution is now relatively slow, the micelles do not adsorb directly, and the adsorption rate is retarded by the slow exchange process. We estimated the micellar relaxation time, i.e., the time a micelle needs to break up. For the largest polymer we found that the relaxation time was in the order of a few tens of seconds. The other polymers have a micellar relaxation time that is shorter than roughly one second.

In the initial regime of the adsorption curve the adsorption rate is diffusion limited (for the three smallest polymers) or exchange rate limited (for the largest polymer). This leads to a linear increase of the adsorption as a function of time. When the brush begins to develop, a steric barrier is created for new incoming polymer molecules. In principle, this could give rise to rather slow adsorption kinetics. However, on silica we find adsorption curves with a rather fast transition from the (second) linear regime to the plateau. For titania the transition is more gradual, which points to a higher barrier for the adsorption. This is a surprising result, because one would expect the barrier to be independent of the adsorption energy. The adsorbed amounts in the plateau of the adsorption curves are very high, as expected for strongly adsorbing diblock copolymers with a relatively short anchor block. The adsorption kinetics of the largest polymer is very slow; in this case the equilibrium adsorbed amount is probably not reached within the time scale of the measurements (up to several hours). The adsorbed amount on silica is considerably higher than on titania. The PDMS block is anchored more strongly to the silica surface, so that the brush density can become higher than on titania. Upon dilution with water, the three largest polymers do not desorb at all; only the shortest polymer molecule (with only 7 anchor segments) shows a considerable desorption. The desorption from titania is higher than from silica, in line with the lower adsorption energy on the former surface.

Acknowledgment. We acknowledge Dr. J. S. Riffle, Virginia State University, for providing the diblock copolymer samples. Dr. P. M. Frederik and Mr. P. H. H. Bomans, University of Limburg, The Netherlands, kindly performed the TEM measurements. We thank Mr. M. C. P. van Eijk for very helpful in discussions on the theory of adsorption kinetics from micellar solutions. This project was financed by the Dutch Ministery of Economic Affairs under the Innovative Research Program (IOP) on paints.

References and Notes

(1) Fleer, G. J.; Cohen Stuart, M. A.; Scheutjens, J. M. H. M.; Cosgrove, T.; Vincent, B. *Polymers at Interfaces*; Chapman & Hall: London, 1993.
(2) Napper, D. H. *Polymeric Stabilisation of Colloidal Dispersions*; Academic Press: London, 1983.
(3) Marques, C. M.; Joanny, J. F.; Leibler, L. *Macromolecules* **1988**, *21*, 1051.
(4) Marques, C. M.; Joanny, J. F. *Macromolecules* **1989**, *22*, 1454.
(5) Van Lent, B.; Scheutjens, J. M. H. M. *Macromolecules* **1989**, *22*, 1931.
(6) Evers, O. A.; Scheutjens, J. M. H. M.; Fleer, G. J. *J. Chem. Soc., Faraday Trans.* **1990**, *86*, 1333.
(7) Johner, A.; Joanny, J. F. *Macromolecules* **1990**, *26*, 5299.
(8) Kopf, A.; Baschnagel, J.; Wittmer, J.; Binder, K. *Macromolecules* **1996**, *29*, 1433.
(9) Amiel, C.; Sikka, M.; Schneider, J. W.; Tsao, Y. H.; Tirrell, M.; Mays, J. W. *Macromolecules* **1995**, *28*, 3125.
(10) Bijsterbosch, H. D.; Cohen Stuart, M. A.; Fleer, G. J.; Van Caeter, P.; Goethals, E. J. *Macromolecules*, in press.
(11) Cosgrove, T.; Zarbakhsh, A.; Luckham, P. F.; Hair, M. L.; Webster, J. R. P. W. *Faraday Discuss.* **1994**, 189.
(12) Guzonas, D.; Hair, M. L.; Cosgrove, T. *Macromolecules* **1992**, *25*, 2777.
(13) Huguenard, C.; Varoqui, R.; Pefferkorn, E. *Macromolecules* **1991**, *24*, 2226.
(14) Munch, M. R.; Gast, A. P. *Macromolecules* **1990**, *23*, 2313.
(15) Parsonage, E.; Tirrell, M.; Watanabe, H.; Nuzzo, R. G. *Macromolecules* **1991**, *24*, 1987.
(16) Tripp, C. P.; Hair, M. L. *Langmuir* **1996**, *12*, 3952.
(17) Tiberg, F.; Malmsten, M.; Linse, P.; Lindman, B. *Langmuir* **1991**, *7*, 2723.
(18) Milner, S. T. *Science* **1991**, *251*, 905.
(19) Halperin, A.; Alexander, S. *Macromolecules* **1989**, *22*, 2403.
(20) Dabros, T.; Van de Ven, T. G. M. *Colloid Polym. Sci.* **1983**, *261*, 694.
(21) Abramowitz, M.; Stegun, I. A. *Handbook of Mathematical Functions*; Dover: New York, 1972.
(22) Liu, Q.; Wilson, G. R.; Davis, R. M.; Riffle, J. S. *Polymer* **1993**, *34*, 3030.
(23) Van Krevelen, D. W. *Properties of Polymers, Their Estimation and Correlation with Chemical Structure*; Elsevier: Amsterdam, 1976.
(24) Brandrup, J.; Immergut, E. H., Eds. *Polymer Handbook*, 3rd ed.; Wiley and Sons: New York, 1989.
(25) Lin, Z.; Hill, R. M.; Davis, H. T.; Scriven, L. E.; Talmon, Y. *Langmuir* **1994**, *10*, 1008.

(26) Bellare, J. R.; Davis, H. T.; Scriven, L. E.; Talmon, Y. *J. Electron. Microsc. Tech.* **1988**, *10*, 87.
(27) Frederik, P. M.; Stuart, M. C. A.; Verkleij, A. J. *Biochim. Biophys. Acta* **1989**, *979*, 275.
(28) Dijt, J. C.; Cohen Stuart, M. A.; Fleer, G. J. *Adv. Colloid Interface Sci.* **1994**, *50*, 79.
(29) Nagpal, V. J.; Davis, R. M.; Liu, Q.; Facinelli, J.; Riffle, J. S. *Langmuir* **1994**, *10*, 4434.
(30) Koppel, D. E. *J. Chem. Phys.* **1972**, *57*, 4814.
(31) Provencher, S. W.; Hendrix, J.; De Maeyer, L.; Paulussen, N. *J. Chem. Phys.* **1978**, *69*, 4273.
(32) Provencher, S. W. *Comput. Phys. Commun.* **1982**, *27*, 213.
(33) Suss, D.; Cohen, Y.; Talmon, Y. *Polymer* **1995**, *36*, 1809.
(34) Mortensen, K.; Talmon, Y. *Macromolecules* **1995**, *28*, 8829.
(35) Chen, C. H.; Wilson, J. E.; Davis, R. M.; Chen, W.; Riffle, J. S. *Macromolecules* **1994**, *27*, 6376.
(36) Chen, C. H.; Wilson, J. E.; Chen, W.; Davis, R. M.; Riffle, J. S. *Polymer* **1994**, *35*, 3587.
(37) Lyklema, J. *Fundamentals of Interface and Colloid Science. I. Fundamentals*; Academic Press: London, 1991.
(38) Cohen Addad, J. P.; Morel, N. *J. Phys. III France* **1996**, *6*, 267.
(39) Dewalt, L. E.; Ouyang, H. D.; Dimonie, V. L. *J. Appl. Polym. Sci.* **1995**, *58*, 265.
(40) Tiberg, F.; Jonsson, B.; Lindman, B. *Langmuir* **1994**, *10*, 3714.

MA971793L